Gastric Cancer
https://doi.org/10.1007/s10120-020-01062-8

ORIGINAL ARTICLE

Phosphoproteomic analysis identifies CLK1 as a novel therapeutic target in gastric cancer

Niraj Babu[1,2] · Sneha M. Pinto[1,3] · Manjusha Biswas[4] · Tejaswini Subbannayya[1,4] · Manoj Rajappa[4] · Sonali V. Mohan[1,2] · Jayshree Advani[1] · Pavithra Rajagopalan[1] · Gajanan Sathe[1] · Nazia Syed[1] · Vinod D. Radhakrishna[4] · Oliyarasi Muthusamy[4] · Sanjay Navani[5] · Rekha V. Kumar[6] · Gopal Gopisetty[7] · Thangarajan Rajkumar[7] · Padhma Radhakrishnan[8] · Saravanan Thiyagarajan[4] · Akhilesh Pandey[1,2,9,10,11] · Harsha Gowda[1,2,12] · Pradip Majumder[8] · Aditi Chatterjee[1,2,4]

Received: 5 June 2019 / Accepted: 12 March 2020

Abstract

Background Phosphorylation is an important regulatory mechanism of protein activity in cells. Studies in various cancers have reported perturbations in kinases resulting in aberrant phosphorylation of oncoproteins and tumor suppressor proteins.
Methods In this study, we carried out quantitative phosphoproteomic analysis of gastric cancer tissues and corresponding xenograft samples. Using these data, we employed bioinformatics analysis to identify aberrant signaling pathways. We further performed molecular inhibition and silencing of the upstream regulatory kinase in gastric cancer cell lines and validated its effect on cellular phenotype. Through an ex vivo technology utilizing patient tumor and blood sample, we sought to understand the therapeutic potential of the kinase by recreating the tumor microenvironment.
Results Using mass spectrometry-based high-throughput analysis, we identified 1,344 phosphosites and 848 phosphoproteins, including differential phosphorylation of 177 proteins (fold change cut-off ≥ 1.5). Our data showed that a subset of differentially phosphorylated proteins belonged to splicing machinery. Pathway analysis highlighted Cdc2-like kinase (CLK1) as upstream kinase. Inhibition of CLK1 using TG003 and CLK1 siRNA resulted in a decreased cell viability, proliferation, invasion and migration as well as modulation in the phosphorylation of SRSF2. Ex vivo experiments which utilizes patient's own tumor and blood to recreate the tumor microenvironment validated the use of CLK1 as a potential target for gastric cancer treatment.
Conclusions Our data indicates that CLK1 plays a crucial role in the regulation of splicing process in gastric cancer and that CLK1 can act as a novel therapeutic target in gastric cancer.

Keywords Phosphoserine/threonine · Spliceosome complex · Targeted therapy · Biomarker · PDX in vivo models

List of abbreviations

CLK	Cdc2-like kinase
PDX	Patient-derived xenografts
IHC	Immunohistochemistry
TMT	Tandem Mass Tag
bRPLC	Basic pH reverse phase chromatography
HCD	Higher energy collision dissociation
IPA	Ingenuity pathway analysis
FBS	Fetal bovine serum

Introduction

Gastric cancer is the fifth most common type of cancer in terms of incidence and third leading cause of cancer related deaths globally [1]. Surgical resection is the predominant curative treatment in addition to traditional radiotherapy and chemotherapy as adjuvant or neoadjuvant therapy [2]. Drugs such as 5-fluorouracil (5-FU) and leucovorin have been frequently used in neoadjuvant chemotherapy in gastric cancer [3, 4]. In addition, viable clinical therapies for gastric cancer

Electronic supplementary material The online version of this article (https://doi.org/10.1007/s10120-020-01062-8) contains supplementary material, which is available to authorized users.

✉ Pradip Majumder
pradipkmajumder@gmail.com

✉ Aditi Chatterjee
aditixchatterjee@gmail.com

Extended author information available on the last page of the article

Published online: 24 April 2020

are limited to targeting of HER2 and VEGFR2 [5]. Sunitinib, which is a tyrosine kinase inhibitor known to target VEGFR, PDFG and FLT3 among others, is known to be of clinical value as a second line of treatment for advanced gastric cancer [6, 7]. FOLFIRI is a well-known chemotherapy regimen primarily used in the treatment of metastatic gastric cancer [8]. However, when sunitinib was administered with FOLFIRI, it did not improve progression-free survival as well as response in chemotherapy-resistant gastric cancer [9]. This calls for the development of an alternative strategy and development of new therapeutic targets for the treatment of gastric cancer.

The preference of patient-derived xenografts (PDXs) in drug development research is because it enables the scale up of the primary tumor and retains stromal elements and near-resemblance to the original tumor in comparison to cell line models [10]. In the current study, we studied the altered signaling in gastric cancer using mass spectrometry-based quantitative phosphoproteome profiling to aid in identifying potential biomarkers to act as therapeutic targets. We compared the phosphoproteome of primary gastric tumor tissue and PDX derived from the same tumor and compared with the adjacent normal tissue for each case.

Analysis of the quantitative phosphoproteomic data revealed altered phosphorylation in splicing proteins. Alternative splicing is a regulated process in gene expression which determines the inclusion or exclusion of coding sequences from the final processed mRNA to yield protein isoforms that vary in their peptide sequence [11]. Abnormal splicing mechanism may increase or decrease protein expression, which in turn, can lead to tumorigenesis [12]. However, amongst the instances of missplicing of mRNAs that have been reported, focus of a large majority of studies is on mutation-based aberrations in spliceosome activity [13]. Studies pertaining to splicing abnormalities due to post-translational modifications such as differential phosphorylation events, are limited, specifically in cancer. Early reports have shown how reversible protein phosphorylation is an important mechanism of positive as well as negative regulation of pre-mRNA splicing [14]. A particular example of phosphorylation-mediated regulation of splicing factors can be seen in a study of Wilms tumor, where phosphorylation of SRSF1 by SRPK1 leads to proangiogenic proteins VEGF165 of the VEGFA being produced [15]. In another example, in non-small cell lung cancer, it has been observed that RAS signaling pathway inducing the hyperactivation of AKT leads to phosphorylation of SRSF1 thus enhancing its promotion of pro-survival splice variants of *KLF-6* and *CASPASE-9* genes [16].

Cdc2-like kinase (CLK1) was identified as a potential modulator of spliceosome protein phosphorylation indicating its essential role in gastric cancer. Our data highlights the significant role of CLK1 in proliferation, invasion and migration in gastric cancer. Using immunohistochemistry (IHC), we have shown significant overexpression of CLK1 in gastric tumor samples compared to normal tissue. In addition, using an ex vivo explant model, in an individualized tumor microenvironment (TME) settings [17], we have further demonstrated the clinical importance of CLK1 as a promising therapeutic target in gastric cancer.

Methods

Establishment of patient-derived xenografts

Solid tumor tissues from three gastric adenocarcinoma cases, along with their adjacent normal tissues were obtained from Kidwai Memorial Institute of Oncology, Bangalore. The study was approved by the ethics committee at Kidwai Memorial Institute of Oncology and informed consent was obtained from all patients.

All mice studies and experimental protocols were duly approved by the institutional animal ethics committee (IAEC). Freshly resected human tumor specimens were transported to the animal facility at Mitra Biotech Private Limited (MBPL), Bangalore. The specimen was washed in normal saline containing antibiotics and then sliced into of ~ 4–5 mm^3. The tumor slices were subcutaneously implanted to the flanks of 4–6 weeks old, female, severe combined immunodeficiency mice (SCID/Beige, Harlan). Tumor growth, health condition and body weights were periodically monitored. Tumor volume was measured using the following formula, Tumor volume (mm^3) = (π/6) LWH, where *L* length (mm), *W* width (mm) and *H* height (mm) as described previously [17] (Supplementary Fig. 1a).

TMT labeling

For quantitative phosphoproteomics experiment, a total of 9 samples were used—3 gastric cancer tissue samples, 3 case-matched adjacent normal gastric tissue samples, and 3 case-matched xenograft samples. The digested samples were labeled using TMT 10-plex reagent kit (Thermo Scientific, Bremen, Germany) as described previously [18]. Digested proteins derived from the three adjacent normal gastric tissue were labeled with TMT labels, 127N, 128C and 130N, and the case-matched gastric tumor were labeled with 127C, 129N, and 130C and PDX protein samples were labeled with 128N, 129C and 131, respectively. The labeled samples were pooled and loaded on a Sep-Pak C18 column (Waters, Milford, MA) equilibrated with 0.1% trifluoroacetic acid (TFA). Washed peptides were eluted using 0.1% TFA and 40% acetonitrile (ACN) and subject to lyophilisation. The lyophilized samples were reconstituted in 7 mM TEABC (pH 9, solution A) and basic pH reverse phase chromatography

(bRPLC) was carried out as described previously [19]. The bRPLC fractions were pooled to obtain 12 fractions. Further sample preparation details, including phosphopeptide enrichment, LC–MS/MS parameters, and data analysis are provided in Supplementary Methods.

Cell culture

Gastric cancer cell lines—SNU-1, SNU-5, SNU-16, KATO-III and AGS, were procured from ATCC (Manassas, VA). All cell lines were grown in RPMI-1640 medium (Invitrogen; Carlsbad, CA) supplemented with 10% fetal bovine serum (FBS) and maintained in a humidified CO_2 incubator at 37 °C.

siRNA transfection

ON-TARGETplus SMARTpool CLK1 siRNA and control siRNA were purchased from Dharmacon (Lafayette, CO). Gastric cancer cells were transfected with control and CLK1 siRNA using RNAiMAX reagent (Invitrogen, Carlsbad, CA) as per the manufacturer's instructions.

Cell viability assays

Each cell line was seeded in a 96-well plate at the seeding density of 8×10^3 per well and incubated overnight in a humidified CO_2 incubator. The cells were treated with different concentrations (1 µM, 5 µM and 10 µM) of CLK inhibitor, TG003 (catalog# S7320, Selleckchem, Houston, TX) in normal growth media and incubated for 48 h, followed by the addition of 3-(4,5-dimethylthiazol-2-yl)-2,5-diphenyltetrazolium bromide (MTT) reagent. Cell viability was assessed by measuring absorbance at 570 nm and 650 nm. Each treatment was carried out in triplicate and the mean value of cell viability was measured and compared against the viability of cells treated with DMSO (control). Paired *t* test was carried out to evaluate the difference between the control and treated groups. P value < 0.05 was considered to be significant.

Cell proliferation assays

Cell proliferation assays were carried out as described previously [20]. Cells were seeded in a 96-well plate followed by overnight incubation. Each cell line was then treated with TG003 (10 µM) or 20 nM CLK1 siRNA for a maximum duration of 96 h and 72 h, respectively. MTT assay was performed to determine cell proliferation by measuring the absorbance at 570 nm and 650 nm. All experiments were carried out in triplicate and repeated thrice. Paired *t* test was carried out to evaluate the difference between the control and treated groups. P value < 0.05 was considered to be significant.

Cell invasion assays

Cell invasion assays were carried out using a transwell system (BD Biosciences, San Jose, CA). Inner surface of the filter was coated with Matrigel (BD Biosciences, San Jose, CA), as described previously [21]. Cells were treated with TG003 (10 µM) or 20 nM CLK1 siRNA and seeded in the transwell at a density of 2×10^4 cells/insert in 500 µl of serum-free media. The transwell system was then placed in a 24-well plate in complete media and incubated at 37 °C in 5% CO_2 incubator for 48 h. Post-incubation, the transwell was removed and the inner surface of the well was wiped using a cotton-tip applicator to remove non-migratory cells. The invaded cells on the lower surface of the membrane was fixed with methanol and stained using 4% methylene blue (Sigma, St. Louis, MO). For non-adherent cells, invasion was assessed by counting the number of cells that migrated into the serum-rich media within the culture plate. Each experiment was carried out in triplicate and repeated thrice. Representative images were photographed at 10× magnification. Paired *t* test was carried out to evaluate the difference between the control and treated groups. P value < 0.05 was considered to be significant.

Colony formation assays

Colony forming ability was assessed using AGS gastric cancer cell lines as described earlier [22]. Briefly, 3×10^3 cells were seeded into a 6-well plate and treated with CLK1 inhibitor, TG003 (10 µM) or CLK1 siRNA in complete media. The cells were observed for a period of 8–10 days. After the desired period of treatment, media was removed and cells were fixed with methanol and stained with 4% methylene blue (Sigma, St. Louis, MO). Cells were observed under a microscope and colonies formed were counted in ten randomly chosen microscopic fields. All experiments were conducted in triplicates and repeated thrice. Representative images were photographed at 2.5× magnification. Paired *t* test was carried out to evaluate the difference between the control and treated groups. P value < 0.05 was considered to be significant.

Wound healing assays

AGS cells were seeded in 6-well plate at a density of 1×10^5 cells/well and incubated until 85% confluency was attained. This was followed by introduction of a scratch wound as described previously [23]. Cells were washed with phosphate buffered saline (PBS) to remove cell debris followed by addition of growth media supplemented with 10% FBS

with CLK1 inhibitor TG003 (10 µM) or 20 nM CLK1 siRNA. Cells were incubated in a humidified 5% CO_2 incubator at 37 °C for 20 h and imaged at 0 h and 20 h after treatment. All experiments were carried out in triplicates and repeated thrice. The wound migration was assessed using ImageJ software [24] and compared relatively with the migration of control cells incubated for the same time duration. Representative images were photographed at 10× magnification. Paired *t* test was carried out to evaluate the difference between the control and treated groups. *P* value < 0.05 was considered to be significant.

Western blot

Whole cell extracts of gastric cancer cells were prepared using modified RIPA lysis buffer (Merck Millipore, Billerica, MA) containing protease inhibitors (Roche, Indianapolis, IN) and phosphatase inhibitors (Thermo Scientific, Bremen, Germany). 30 µg of protein from each condition was used for western blot. Proteins were resolved on acrylamide gel and hybridized on nitrocellulose membrane which were probed with primary antibodies, and developed using Luminol reagent (Santa Cruz Biotechnology, Dallas, TX). Anti-CLK1 (catalog# 209681) and anti-SRSF2 (catalog# 204916) primary antibodies were obtained from Abcam (Cambridge, MA). Anti-Phospho-AKT (S473) (catalog# 4058) and anti-AKT (catalog# 9272) antibodies were obtained from Cell Signaling Technologies, Beverly, MA). Anti-phospho-SRPK2 (catalog# 71817; Millipore, Burlington, MA), anti-SRPK2 (catalog# 611118; BD Biosciences, San Jose, CA). β-Actin antibody (catalog# A5316; Sigma, St. Louis, MO) was used a loading control. ImageJ software was used to obtain densitometry of the resultant bands [24].

CANscript culture

To study the ex-vivo response of CLK1 inhibition on tumor, the PDX samples were manually dissected to the explant size of 2–3 mm^3. These explants were randomized in the culture to ensure tumor heterogeneity. The explants were cultured either in triplicate or quadruplicate as described previously [25] in the individualized microenvironment. The cultured xenograft explants were maintained for 72 h, with either TG003 (10 µM), fluorouracil (5-FU, 16.78 µg/ml) or leucovorin (391 ng/ml) individually or in combination, along with vehicle controls (DMSO) which was replaced every 24 h. The cultures were harvested at the end of 72 h (T72), fixed with 10% formalin and paraffin embedded for histopathology assessment. Detailed methodology of the immunohistochemistry experiment has been provided in Supplementary Methods.

S-score generation

Values from histology (morphology), tumor cell proliferation, cell death and viability were used as inputs in a machine learning algorithm as described earlier [17, 26]. The algorithm finally generates a single score (S-score) which has the potential of predicting clinical outcome to therapy. A value greater than 19.1 may clinically correspond with response to the drug(s) tested in CANscript, while a value lower or equal to 19.1 may indicate non-response. S-score was generated for the drug arms tested in CANscript.

Statistical analysis

Statistical analysis for the calculation of *P* value was carried out using Student's *t* test in Perseus software [27].

Results

Phosphoproteomic dysregulation in gastric cancer

We carried out TMT labeling-based proteomic analysis coupled with phospho-Ser/Thr enrichment to identify differentially phosphorylated proteins in gastric tumor and PDX samples, compared to adjacent normal tissue (Supplementary Fig. 1b). We identified 1,344 phosphosites belonging to 848 proteins common in both tumor and PDX samples. A total of 85 proteins were hyperphosphorylated (fold change ≥ 1.5) and 92 proteins were hypophosphorylated (fold change ≤ 0.6) in common between gastric tumor and PDX samples compared to adjacent normal tissue (Fig. 1a). The phosphosite distribution identified in this study is provided in Fig. 1b. Complete list of proteins identified in this study are provided in Supplementary Table 1.

Functional annotation of differentially phosphorylated proteins using IPA resulted in the enrichment of splicing mechanism as one of the top hits (Fig. 1c). We identified several hyperphosphorylated proteins in our proteomic data pertaining to mRNA processing and splicing machinery (Supplementary Table 2). Among the hyperphosphorylated proteins, we identified proteins which belonged to the mRNA splicing machinery. For example, SRSF1 and SRSF2 were known to enhance U1 snRNP binding to 5′ splice site along with U2 snRNP binding to 3′ splice site [28, 29], along with bridging the interaction between preliminary splice site recognition events in pre-spliceosome and mature spliceosome [30]. Similarly, RBM39 is postulated to modulate alternate splicing through direct interaction with RNA or recruitment of other splice factors like U2AF65 [31]. Pathway analysis and literature survey identified CLK1 as an upstream kinase regulating the activity of proteins including SRPK1, SRSF1, SRSF2 and SRSF6

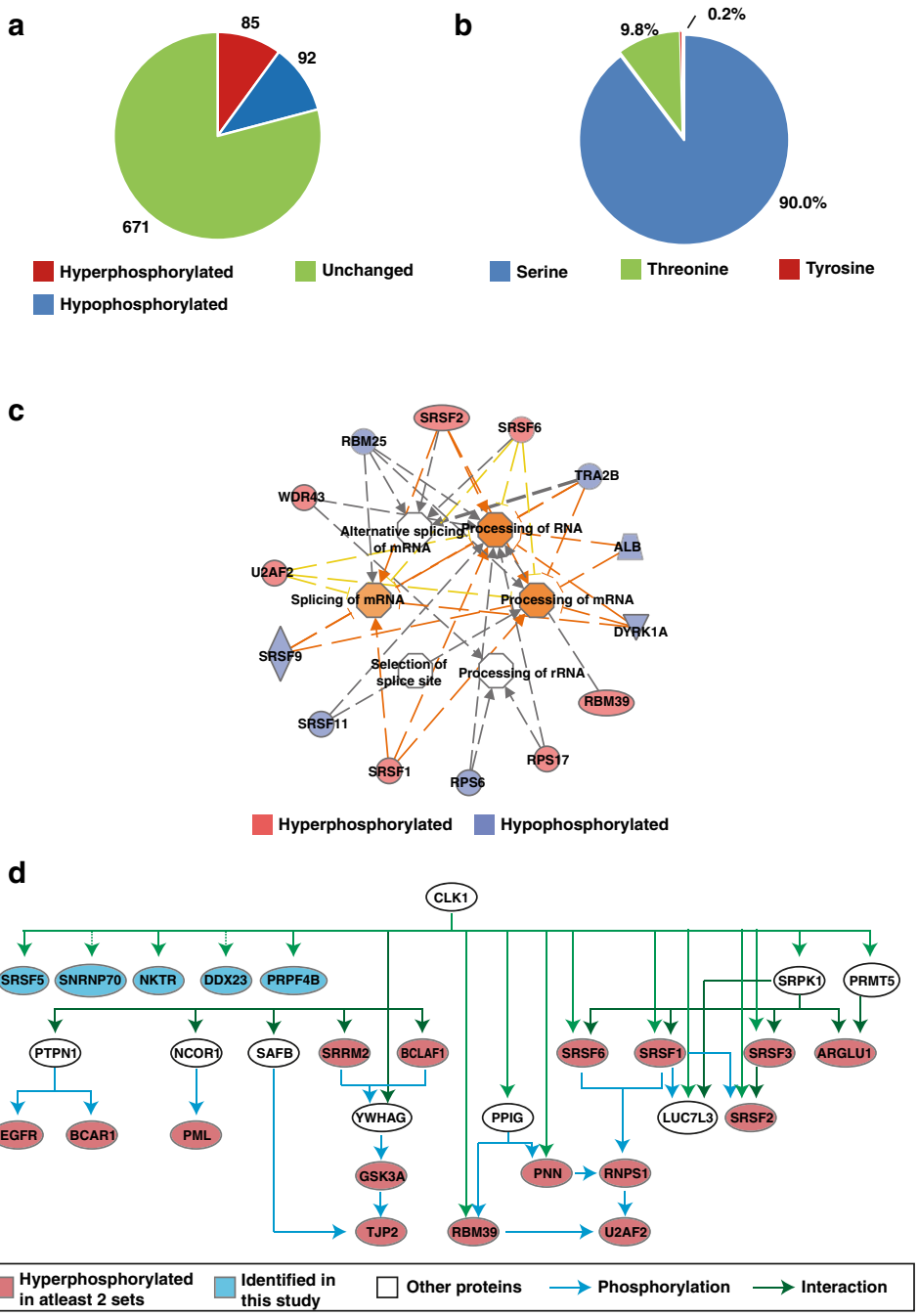

Fig. 1 Phosphoproteomic analysis of gastric cancer. **a** Pie-chart depicting the distribution of differentially phosphorylated proteins gastric cancer samples compared to adjacent normal tissue. **b** Pie-chart depicting the distribution of phosphorylation sites across differentially phosphorylated proteins in gastric cancer. **c** Network of pathways enriched by differentially phosphorylated proteins in gastric cancer identified using IPA. **d** Interaction network displaying proteins of the spliceosome machinery which were identified and/or quantified in this study. Direct and indirect targets of CLK1 are shown in solid and dotted lines, respectively

(Fig. 1d). Supplementary Fig. 2a provides hierarchical clustering of total and phosphoprotein expression of the spliceosome complex proteins differentially phosphorylated in this data. Representative MS/MS spectra of a few spliceosome complex proteins identified in this study are provided in Supplementary Fig. 2b–d.

CLK1 is essential for viability of gastric cancer cells

As our proteomic data indicate dysregulation of splicing proteins, which are downstream of the kinase CLK1, we sought to study the role of CLK1 in the pathobiology of gastric cancer. To study the effects of CLK1 inhibition on cell viability, gastric cancer cell lines were treated with varying concentrations of the CLK1 inhibitor, TG003 (1, 5, 10 μM). 1 μM concentration of TG003 did not show any significant decrease in cell viability. Both 5 μM and 10 μM concentrations of TG003 resulted in significant decrease in cell viability. However, the viability of SNU-5, SNU-16, KATO-III and AGS were less than 50% upon treating the cells with 10 μM TG003 (Supplementary Fig. 3). All

further assays were carried at 10 μM concentration, unless otherwise mentioned.

After the optimum dose of TG003 for cell viability was determined, we evaluated the effect of CLK1 inhibition on the proliferation of gastric cancer cells for every 24 h up to 96 h. Inhibition of CLK1, using 10 μM TG003 or 20 nM CLK1 siRNA, resulted in a significant decrease in cellular proliferation of gastric cancer cells compared to untreated control cells (Fig. 2a, b). We observe a significant difference in cellular proliferation after 48 h of treatment with TG003 and CLK1 siRNA (p value < 0.05) and continued to observe decreased proliferation till the experiment was terminated (p value < 0.05).

In addition to proliferation, inhibition of CLK1 also led to significant decrease in the colony forming ability of gastric cancer cell line (p value < 0.05). We observed a six-fold decrease in the number of colonies formed in AGS cell line treated with 10 μM TG003 and CLK1 siRNA compared to control (Fig. 3a–d). As the other cell lines used in this study were suspension lines, we could not perform colony

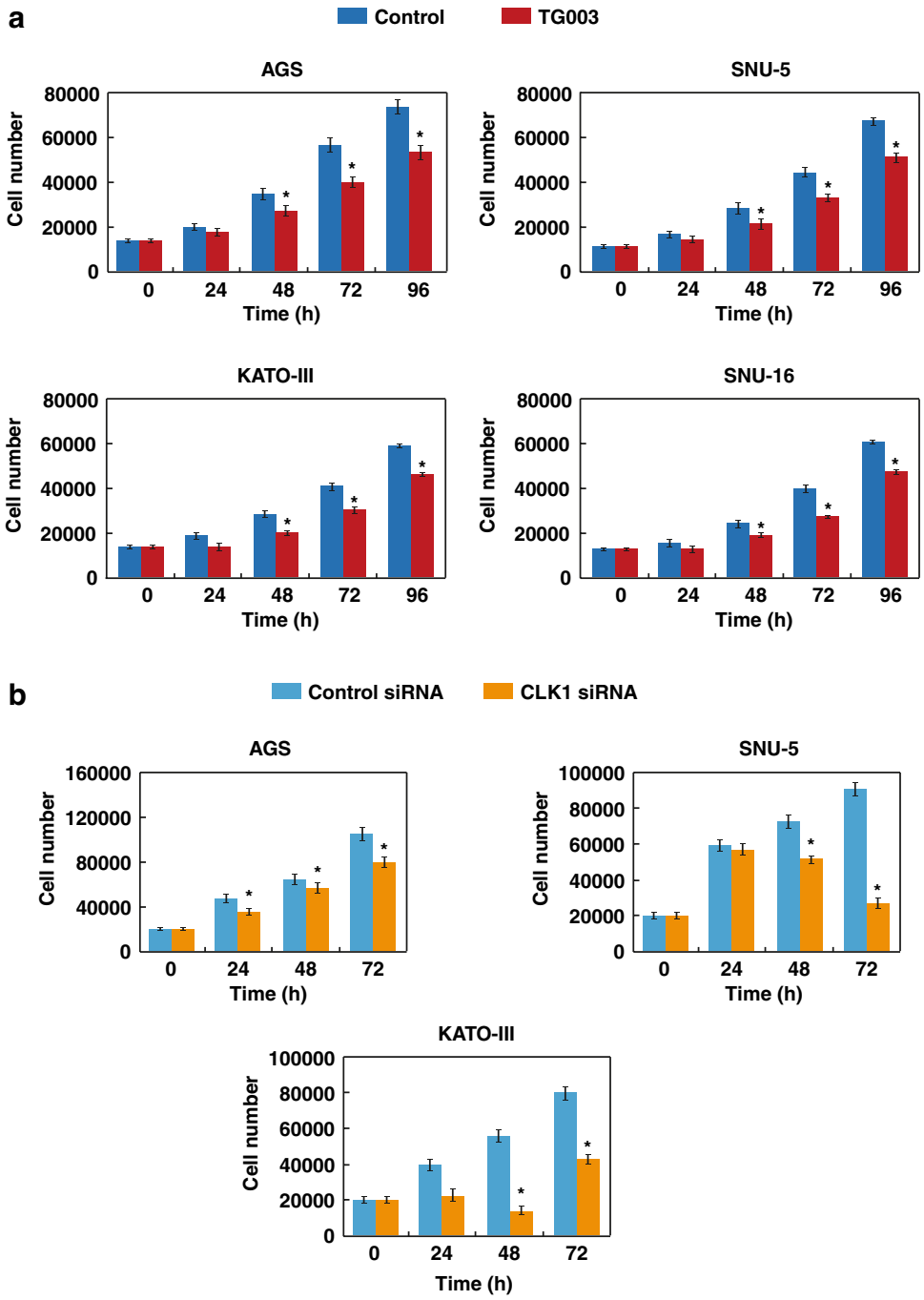

Fig. 2 CLK1 inhibition leads to decreased growth of gastric cancer cell lines. Cellular proliferation of gastric cancer cells on inhibition with **a** CLK1 inhibitor TG003 (10 μM) and **b** CLK1 siRNA (20 nM) (*$p < 0.05$)

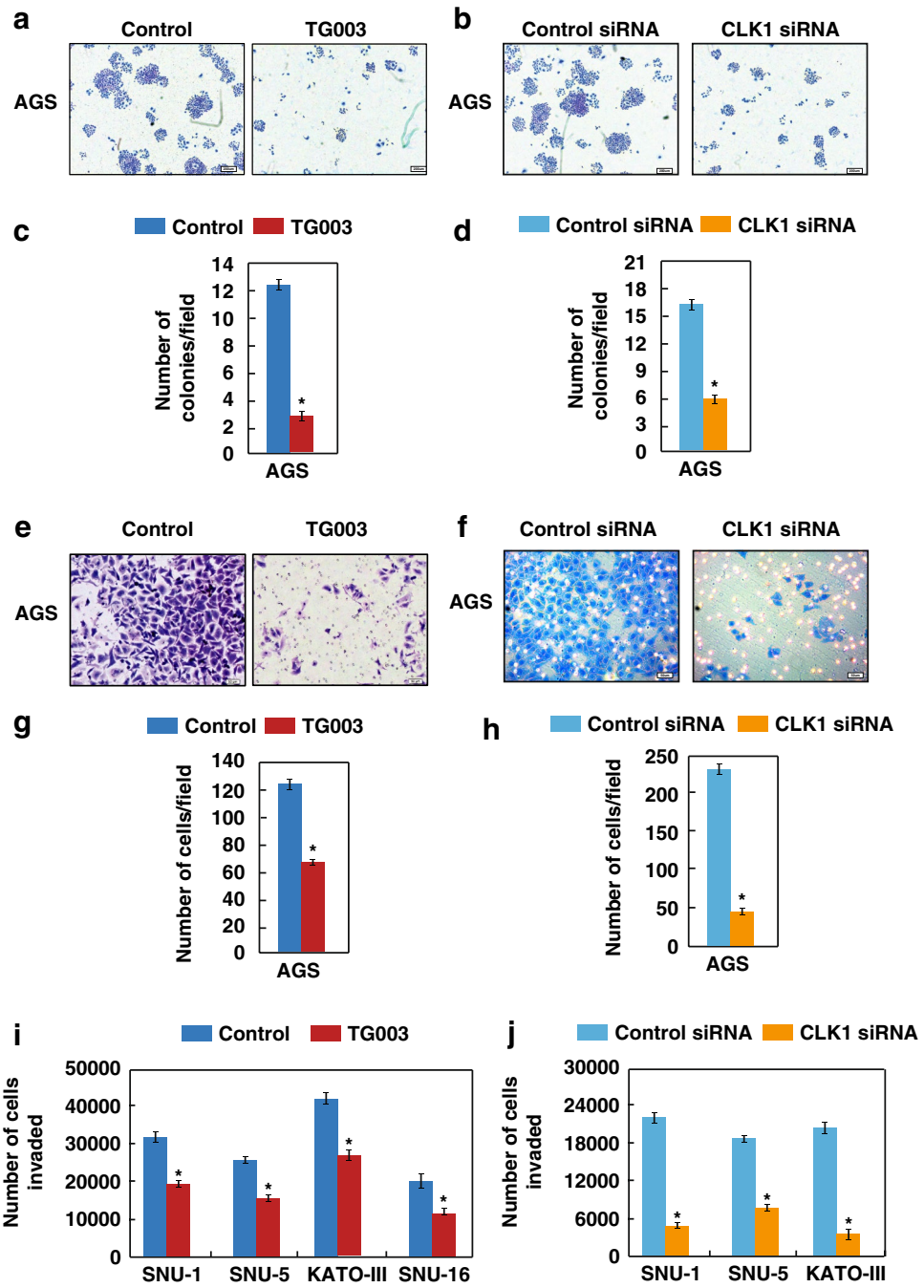

Fig. 3 CLK1 inhibition reduces colony formation and invasiveness of gastric cancer cell lines. **a** Colony formation assay of gastric cancer cell line AGS following the treatment with 10 µM TG003 compared with untreated control cells. **b** Colony formation assay of AGS following the treatment with CLK1 siRNA (20 nM) compared with control siRNA. Colonies formed were visualized upon staining with methylene blue. Scale bar 200 µm. **c** Graphical representation of the colony forming assay using 10 µM TG003 (*$p < 0.05$). **d** Graphical representation of the colony forming assay using 20 nM CLK1 siRNA (*$p < 0.05$). **e** Invasion assay of AGS following treatment with TG003 compared with untreated control cells. **f** Invasion assay of AGS following treatment with CLK1 siRNA compared with control siRNA. Cells that invaded through the Matrigel-coated filters of transwell system were visualized by methylene blue staining and counted. Scale bar 50 µm. **g** Graphical representation of invasive ability of AGS upon treatment with 10 µM TG003 compared with untreated control cells (*$p < 0.05$). **h** Graphical representation of invasive ability AGS upon treatment with 20 nM CLK1 siRNA compared with control siRNA (*$p < 0.05$). **i** Graphical representation of invasive ability of suspension gastric cancer cell lines upon treatment with 10 µM TG003 compared with untreated control cells. **j** Graphical representation of invasive ability of suspension gastric cancer cell lines upon treatment with 20 nM CLK1 siRNA compared with control siRNA (*$p < 0.05$). Cells that invaded through the Matrigel-coated transwell were visualized under microscope and counted

forming assay with those. Taken together, our data indicate that CLK1 plays a significant role in the proliferative ability of gastric cancer cells.

CLK1 inhibition reduces invasive and migratory ability of gastric cancer cell lines

Decreased colony formation ability is often associated with decreased invasion capabilities of cancer cells [32]. The effects of CLK1 inhibition on the invasive ability of gastric cancer cells was studied using transwell assay technique [21]. For AGS, which is an adherent cell line, invasiveness was measured based on the number of cells migrated and adhered to the outer surface of the transwell filter. For non-adherent cell lines, SNU-1, SNU-5, SNU-16 and KATO-III, the number of cells that migrated through the Matrigel-coated insert into the serum-rich media was counted. Inhibition of CLK1 resulted in a significant decrease in the invasive ability of the gastric cancer cells (p value < 0.05). In AGS, we observed almost 40–50% reduction in invasive ability of the cells in TG003 or CLK1 siRNA-treated cells compared to control (Fig. 3e–h). Similarly, the number of cells from the suspension lines which invaded the transwell membrane were significantly reduced upon the inhibition of CLK1 (Fig. 3i, j) (p value < 0.05). The effect of CLK1 inhibition on cellular migration was studied using AGS. Over a period of 20 h, we observed a significant decrease in the migration ability of AGS cells due to inhibition of CLK1 by almost 40% (p value < 0.05) (Fig. 4a–d).

CLK1 regulates expression of spliceosome proteins in gastric cancer

Using cellular assays, we were able to demonstrate that inhibition of CLK1 resulted in decreased proliferation, invasion and migration of gastric cancer cell lines. We further sought to study the potential signaling mechanism of CLK1 in gastric cancer cells. CLK1 has been reported earlier to be involved in the regulation of the spliceosome complex proteins in ovarian cancer and glioma [33, 34]. In addition, inhibition of CLK1 using TG003 has been reported to hinder CLK1-dependent SRSF2 splicing activity in HeLa cells [35].

Western blot analysis revealed a decreased expression of CLK1 in AGS cells on treatment with TG003 or CLK1 siRNA (p value < 0.05). In addition, CLK1-inhibited cells not only led to a decreased expression of splicing protein SRSF2 and pSRPK2 but also pAKT (p value < 0.05) (Fig. 5a–d).

Since AKT is a known upstream regulator of CLK1 [36–38], we also studied the effect of inhibition of AKT on the expression of CLK1, SRSF2 and pSRPK2. Our data indicates that inhibition of AKT led to a decreased expression of CLK1, SRSF2 and pSRPK2 (p value < 0.05). Taken together, our data indicate that CLK1 and AKT signaling may be independent of each other, or a feedback mechanism exists between CLK1 and AKT, where inhibition of any one molecule affects the other, thereby affecting the oncogenic phenotype. However, further validation is required to establish this, which is beyond the scope of this manuscript.

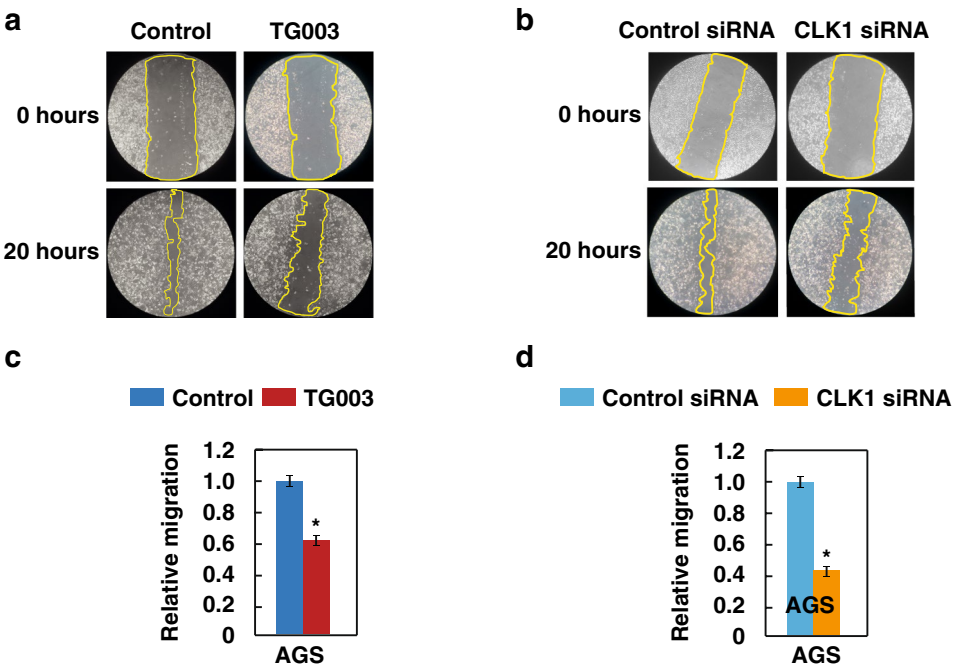

Fig. 4 CLK1 inhibition affects migration ability of gastric cancers. **a** Migration assay of gastric cancer cell line AGS upon treatment with 10 μM TG003 compared with untreated control cells. **b** Migration assay of gastric cancer cell line AGS upon treatment with 20 nM CLK1 siRNA compared with control siRNA. **c** Graphical representation of migratory ability of AGS treated with 10 μM TG003 compared with untreated control cells (*$p < 0.05$). **d** Graphical representation of migratory ability of AGS treated with 20 nM CLK1 siRNA compared with control siRNA (*$p < 0.05$)

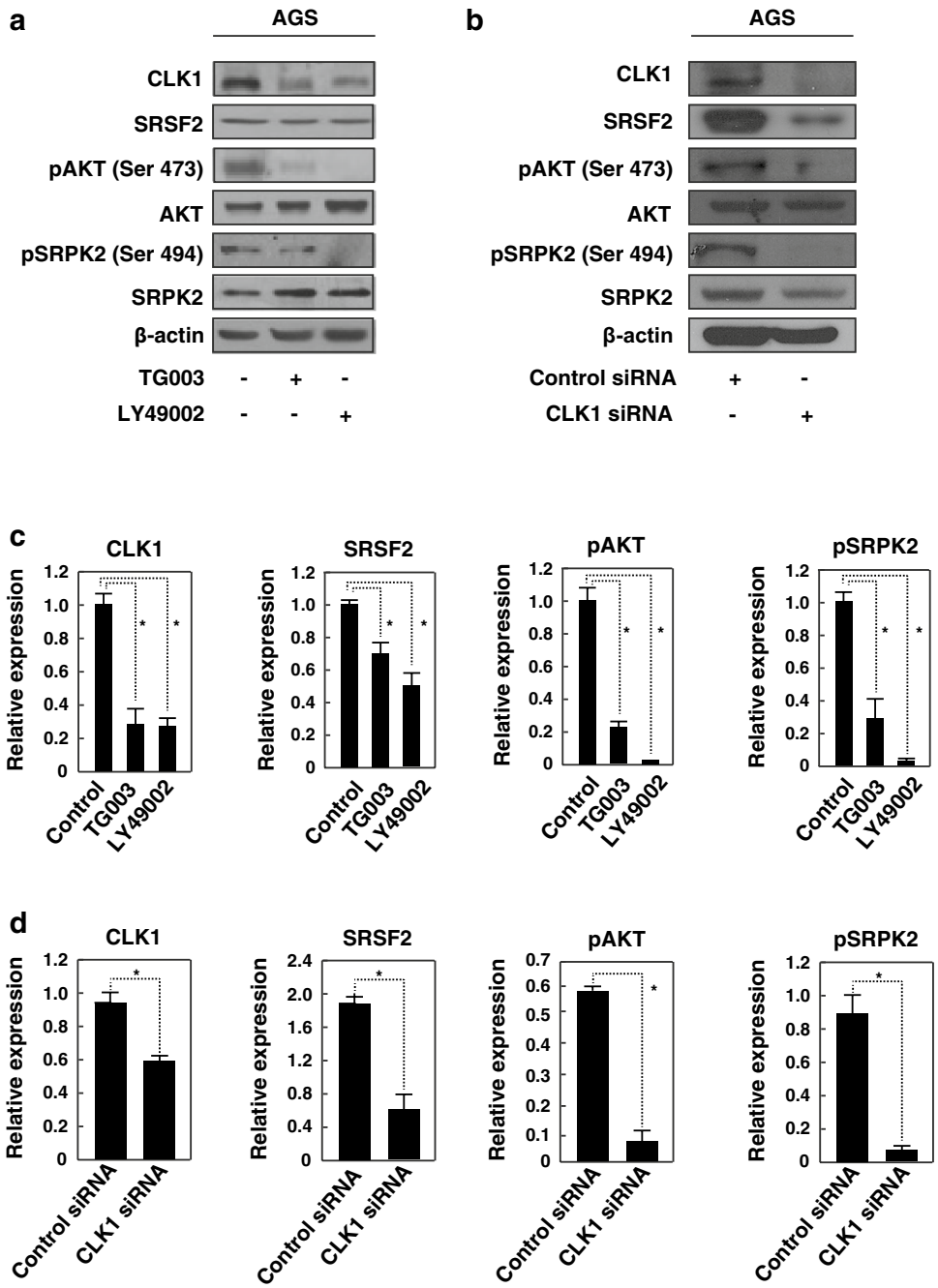

Fig. 5 CLK1 regulates expression of spliceosome proteins in gastric cancer. **a** Western blot of gastric cancer of the indicated proteins using AGS cell line upon treatment with molecular inhibitors of CLK1 (10 μM TG003) and AKT (10 μM LY49002) compared with untreated control. β-Actin was used as loading control. **b** Western blot of the indicated proteins using AGS cell line upon treatment with 20 nM CLK1 siRNA compared with control siRNA. β-Actin was used as loading control. **c** Densitometry graphs representing the relative expression of CLK1, SRSF2, phospho-AKT and phospho-SRPK2 in gastric cell line AGS treated with molecular inhibitors of CLK (10 μM TG003) and AKT (10 μM LY49002) compared with untreated control (*$p < 0.05$). **d** Densitometry graphs representing the relative expression of CLK1, SRSF2, phospho-AKT and phospho-SRPK2 in gastric cell line AGS treated with 20 nM CLK1 siRNA compared with control siRNA (*$p < 0.05$)

Expression of CLK1 in gastric cancer tissue

We next assessed the expression status of CLK1 in primary gastric adenocarcinoma tissues using tissue microarray-based immunohistochemical analysis in 118 cases of gastric cancer. CLK1 staining showed predominantly cytoplasmic localization. Thirty eight percent (36 out of 94) of the gastric cancer tissues showed moderate to strong staining while ninety five percent the normal gastric cores (82 out of 86) which revealed weak to negative staining. The percentage distribution of CLK1 expressed in gastric tumor samples ranged predominantly between 10 and 30%, whereas the expression of CLK1 in normal gastric tissue was mostly below 10%. A Chi-square test confirmed that the overexpression of CLK1 in gastric tumor tissues was statistically significant (p value < 0.0001). In addition, it was observed that tumor tissue cores which showed weak CLK1 staining were of mucinous in nature. Representative staining patterns for CLK1 in gastric and adjacent normal tissue are provided in Fig. 6a. Figure 6b provides

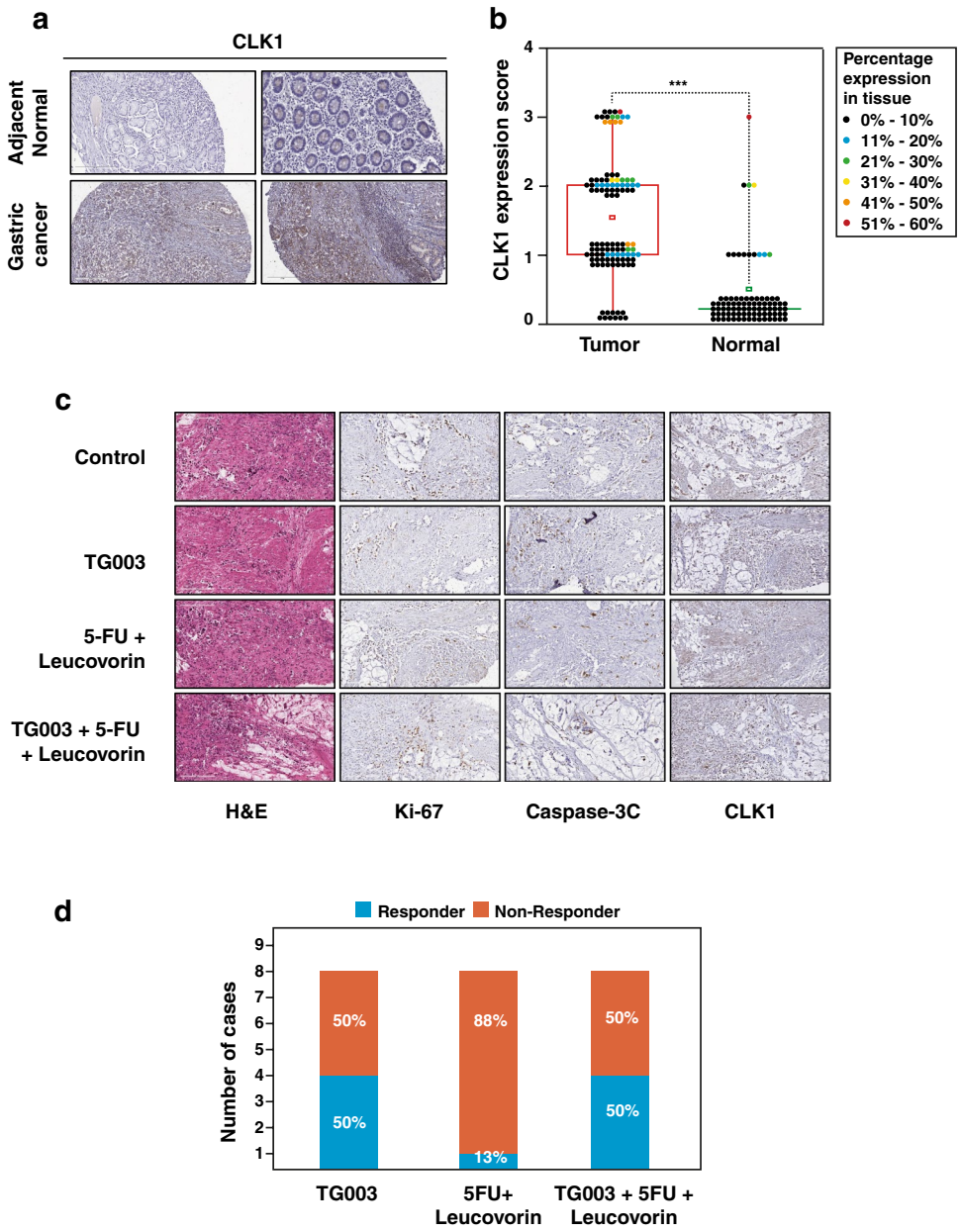

Fig. 6 Expression of CLK1 in gastric cancer tissue. **a** Immunohistochemistry staining of primary gastric cancer tissue representing the expression of CLK1 in gastric cancer tissues and adjacent normal tissues. Scale bar 200 µm. **b** Box-dot plot representing the expression of CLK1 in gastric cancer samples in the tissue microarray. The dots represent the number of samples scored and the color codes represent the percentage CLK1 expression in each sample (*** *p*-value < 0.001). *Y*-axis represents the scores assigned based on the expression of CLK1 in tissue samples. **c** CANscript assay representing the efficacy of targeting CLK1 compared to chemotherapeutic drugs. Representative histological and immunohistochemical staining of gastric cancer explant samples of a responder demonstrating tumor content (H&E), proliferation (Ki-67) and viability (Caspase-3C) upon treatment with different drugs have been shown in the panels. Scale bar 200 µm. **d** Bar graph representing the percentage of gastric cancer cases responding to treatment with CLK1 inhibitor (10 µM TG003) individually and in combination SOC regime used in clinics (5-FU and leucovorin)

a graphical representation depicting the expression score of CLK1 and the number of gastric cancer cases they were detected in. The results of the IHC validation are summarized in Table 1.

Table 1 Summary of the immunohistochemical validation for CLK1 in gastric cancer and normal tissues

Expression score	Tumor tissues	Normal tissues
0–1 + (negative–weak)	58	82
2+ to 3+ (moderate–strong)	36	4
p value of expression	< 0.0001	
Subcellular location of staining	Predominantly cytoplasmic	

Evaluation of CLK1 inhibition using primary gastric cancer tissue

Tumor samples were analysed on a personalized tumor explant culture system (CANscript™) to predict response to CLK1 inhibitor TG003, and one of the standard of care (SOC) options in treatment of gastric cancer, 5-FU and leucovorin.

Patient-derived tumor samples were used in explant culture and were treated with 10 µM of TG003, 16.78 µg/ml of 5-FU and 391 ng/ml of leucovorin, individually and/or in combination. The efficacy of the molecular inhibitor was graded based on assessing phenotypic characteristics such as the viability, tumor content (H&E), proliferation (Ki-67)

and cell death (Caspase 3C) to generate S-score for each tumor tissue. In addition, the HER2 expression of the tissue samples were also assessed to identify correlation between HER2 status and efficacy of treatment. Our data demonstrated that 4 out of 8 tumors categorized to be responders (S-score > 19.1) to CLK inhibitor TG003. We also noticed that treatment with TG003 resulted in better response compared to 5-FU and leucovorin, which is one of the SOC options used in the clinics. In total, 50% of the cases studied were predicted to be responder to TG003 and the combination arm (TG003 + 5-FU + leucovorin), compared to 5-FU and leucovorin where the response rate was only 13%. Three cases did not respond to any treatment arm (samples 3, 4, 7). Sample 4 did not respond to TG003, but responded to the combination therapy, whereas sample 3 responded to TG003 but not to the combination therapy. Sample 1, 5 and 8 responded to both TG003 and the combination therapy. At this juncture, we are unable to comment on the mechanism behind the response pattern of each tumor to the treatment arms. S-scores generated against each treatment arm for the tumor samples has been listed in Table 2. A representative histological staining of a gastric tumor explants (Sample 1) treated with TG003, 5-FU and leucovorin and their combination is presented in Fig. 6c. Supplementary Fig. 4a, b represent histological staining of tumor explants from Sample 2 and 3, respectively, which show a clear distinction in response to treatment with TG003 and in combination with 5-FU and leucovorin. A graphical depiction of the number of responders in each treatment arm is provided in Fig. 6d. Our data indicates a favorable response pattern to TG003 in gastric cancer, as predicted in CANscript. We did not find any correlation between the HER2 status and CLK1 response profile for the gastric cancer samples evaluated in CANscript.

Table 2 Cumulative analysis representing the S-scores for gastric cancer patient samples with TG003 individually and in combination with chemotherapeutic drugs

Sample ID	S-score			HER2 status
	TG003	5-FU + leucovorin	TG003 + 5-FU + leucovorin	
Sample 1	24	25	20	3+
Sample 2	8	7	4	2+
Sample 3	21	7	1	Negative
Sample 4	5	7	22	1+
Sample 5	22	13	20	3+
Sample 6	17	6	17	3+
Sample 7	8	8	3	3+
Sample 8	41	16	45	1+

Discussion

Aberrantly activated signaling events in cancer can often be traced to dysregulation of kinases. This, in turn, results in abnormal activation or repression of the downstream substrates as a result of their differential phosphorylation. Studying the global phosphoproteomic profile and identifying such dysregulated kinases has gained importance in cancer research in recent years [39]. Identification of altered phosphorylation using mass spectrometry have been widely studied in lung [40], ovarian [41] and breast [42] cancers. However, high-throughput phosphoproteomic studies of gastric cancer are few and are mostly restricted to cell line-based investigations [43, 44]. A recent study showed phosphoproteomic analysis of gastric cancer xenografts to identify biomarkers indicating ischemic changes of tumor tissues [45]. Likewise over the years, many studies have indicated the advantages of using patient-derived tumor xenografts over cancer cell lines to study the disease including gastric cancer, due to their ability to mimic tumor complexity and microenvironment [46–49]. In this study, we have carried out TMT-based phosphoproteomic analysis of gastric cancer tissue and xenograft samples to identify differentially phosphorylated proteins which can serve as potential therapeutic targets in gastric cancer.

In this study, we identified molecules belonging to the mRNA processing and alternative splicing machinery such as DYRK1A, SRSF1, SRSF2, SRSF6 and SRSF9 to be hyperphosphorylated [38, 50]. To study the role of splicing proteins in gastric cancer, we examined the phenotypic changes in gastric cancer cell lines by targeting their upstream regulatory kinase, CLK1. CDC-like kinases (CLK) are a family of dual specificity kinase proteins known to phosphorylate splicing factors, thereby regulating their distribution and function within the nucleoplasm [51]. Aberrant activation of splicing factors by CLK1 has been shown to play an important role in cancer [52]. Increased hyperphosphorylation of splicing factor SPF45 by CLK1 was shown to correlate with increased cellular invasion and migration in ovarian cancer cells [33]. Regulation of CLK1 activity by alternative splicing of its transcript has been shown to play a role in predicting prognosis and therapeutic outcome in breast cancer patients [53]. Development of molecular inhibitors of CLK protein kinases, such as TG003, was shown to suppress cell growth and initiate apoptosis in cancer [35, 54]. In addition, CLK1-mediated alternative splicing was also established to be regulated by AKT in 3T3-L1 pre-adipocytes [55]. In addition to TG003, other molecular inhibitors of CLK1, such as the N-benzylated derivative developed by ElHady et al. [56] and the dichloroindolyl enaminonitrile compound developed by Fedorov et al. [57] have been

demonstrated to target CLK1 in cancer cell lines but has been reported to also target CLK4 and DYRK1A [57].

In this study, we demonstrate the importance of CLK1 in regulating alternative splicing proteins as well as the potential of using CLK1 as a therapeutic target in gastric cancer. Through in vitro assays using the molecular inhibitor TG003 and CLK1 siRNA, we were able to demonstrate that targeting CLK1 results in reduced proliferation, invasion and migration of gastric cancer cell lines. In addition, western blot analysis showed that CLK1 inhibition leads to downregulation of SRSF2 expression in gastric cancer cells. This indicates that inhibition of CLK1 leads to deregulation of the spliceosome complex proteins. Dysregulation of the spliceosome proteins has been reported in earlier studies. Recently, studies have demonstrated the importance of SRSF protein kinase 2 (SRPK2) and dual-specificity tyrosine-(Y)-phosphorylation regulated kinase 1A (DYRK1A) hyperphosphorylation in the promotion of head and neck squamous cell carcinoma [18, 38]. CLK1 is known to be upregulated in hypoxia-induced lung cancer [58]. Other splice factor kinases such as SRPK1 are known to be inhibited by SPHINX resulting in decreased tumor growth in prostate cancer [59]. The same study also demonstrates that inhibition of SRPK1 can serve as a potential anti-angiogenic therapy in prostate cancer [59]. Phosphorylation and dephosphorylation of SRSF1 is reported as essential for the assembly of the spliceosome complex [60]. Similarly, phosphorylation of SRSF10 results in the activation of the protein while dephosphorylation results in the repression of splicing activity of the complex [61]. These studies highlight the role of alternative splicing proteins and the aberrations in their activity in promotion of cancer.

Our study highlights the significance of targeting CLK1 as a potential therapeutic candidate in gastric cancer, using the CANscript platform by nurturing the essential components of tumor ecosystem in an individualized setting. Previous studies have demonstrated the impact of such clinically relevant tool in determining the appropriate treatment of choice for a particular patient in the clinic through minimizing the risks associated with the drugs which are not going to benefit the patient [17, 26]. We initially evaluated gastric cancer cell lines to study the anti-tumor potential of specific inhibitor, TG003 at different concentrations. To further understand the clinical relevance of CLK1 in gastric cancer, its expression was evaluated in gastric cancer primary tissues. CLK1 was found to be overexpressed in gastric tissues compared to its normal counterpart. In addition, we employed primary gastric cancer-derived CANscript to assess the therapeutic value of CLK1 using TG003 in comparison with the SOC treatment used in clinics. Based on the S-score generated from the CANscript analysis to recognize responders and non-responders, our study exhibited that targeting CLK1 with its inhibitor TG003 had higher number of responders compared to SOC treatment arm followed in clinics.

In summary, our study highlights the crucial role of spliceosome complex proteins and their dysregulation in gastric cancer. We hypothesize that altered regulation of spliceosome proteins by the upstream kinase CLK1 can be targeted for the development of novel therapy in gastric cancer.

Conclusions

In this study, we demonstrate that oncogenic phenotype in gastric cancer cell lines could be curtailed by targeting CLK1. Our data indicates the potential role of CLK1 in gastric cancer which in turn leads to the activation of alternative splicing proteins including SRPK2. Although the findings of this study elucidate the role of CLK1 as a promising therapeutic target in gastric cancer, we do not rule out the role of other factors that may promote gastric cancer. Furthermore, this study warrants the need of mouse models and ex vivo assay validation on a larger sample size to establish CLK1 as a strong therapeutic target in the treatment of gastric cancer.

Acknowledgements We thank the Department of Biotechnology (DBT), Government of India for research support to the Institute of Bioinformatics (IOB), Bangalore. IOB is supported by DBT Program Support on infrastructure for proteomic data analysis (BT/01/COE/08/05). NB is a recipient of the Senior Research Fellowship from the Council of Scientific and Industrial Research (CSIR), New Delhi, India.

Funding The project was funded with intramural funds of Institute of Bioinformatics and Mitra Biotech.

Compliance with ethical standards

Conflict of interest Manjusha Biswas, Tejaswini Subbannayya, Manoj Rajappa, Vinod D Radhakrishna, Oliyarasi Muthusamy, Padhma Radhakrishnan, Saravanan Thiyagarajan, Pradip Majumder, Aditi Chatterjee are either employees of Mitra Biotech and/or hold equity of Mitra Biotech. The remaining authors declare no competing financial interests.

Ethical approval The study was approved by the ethics committee at Kidwai Memorial Institute of Oncology. Informed consent was obtained from all patients prior to collection of samples. Animal studies and experimental protocols were duly approved by the institutional animal ethics committee (IAEC).

References

1. Ferlay J, Soerjomataram I, Dikshit R, Eser S, Mathers C, Rebelo M, et al. Cancer incidence and mortality worldwide: sources, methods and major patterns in GLOBOCAN 2012. Int J Cancer. 2015;136(5):E359–E386.

2. Schirren R, Reim D, Novotny AR. Adjuvant and/or neoadjuvant therapy for gastric cancer? A perspective review. Ther Adv Med Oncol. 2015;7(1):39–48.
3. Ott K, Sendler A, Becker K, Dittler HJ, Helmberger H, Busch R, et al. Neoadjuvant chemotherapy with cisplatin, 5-FU, and leucovorin (PLF) in locally advanced gastric cancer: a prospective phase II study. Gastric Cancer. 2003;6(3):159–67.
4. Rustum YM. Biochemical rationale for the 5-fluorouracil leucovorin combination and update of clinical experience. J Chemother. 1990;2(Suppl 1):5–11.
5. Apicella M, Corso S, Giordano S. Targeted therapies for gastric cancer: failures and hopes from clinical trials. Oncotarget. 2017;8(34):57654–69.
6. Bang YJ, Kang YK, Kang WK, Boku N, Chung HC, Chen JS, et al. Phase II study of sunitinib as second-line treatment for advanced gastric cancer. Investig New Drugs. 2011;29(6):1449–588.
7. Papaetis GS, Syrigos KN. Sunitinib: a multitargeted receptor tyrosine kinase inhibitor in the era of molecular cancer therapies. BioDrugs. 2009;23(6):377–89.
8. Erdem GU, Bozkaya Y, Ozdemir NY, Demirci NS, Yazici O, Zengin N. 5-Fluorouracil, leucovorin, and irinotecan (FOLFIRI) as a third-line chemotherapy treatment in metastatic gastric cancer, after failure of fluoropyrimidine, platinum, anthracycline, and taxane. Bosn J Basic Med Sci. 2018;18(2):170–7.
9. Moehler M, Gepfner-Tuma I, Maderer A, Thuss-Patience PC, Ruessel J, Hegewisch-Becker S, et al. Sunitinib added to FOLFIRI versus FOLFIRI in patients with chemorefractory advanced adenocarcinoma of the stomach or lower esophagus: a randomized, placebo-controlled phase II AIO trial with serum biomarker program. BMC Cancer. 2016;16:699.
10. Pompili L, Porru M, Caruso C, Biroccio A, Leonetti C. Patient-derived xenografts: a relevant preclinical model for drug development. J Exp Clin Cancer Res. 2016;35(1):189.
11. Black DL. Mechanisms of alternative pre-messenger RNA splicing. Annu Rev Biochem. 2003;72:291–336.
12. Shkreta L, Bell B, Revil T, Venables JP, Prinos P, Elela SA, et al. Cancer-associated perturbations in alternative pre-messenger RNA splicing. Cancer Treat Res. 2013;158:41–944.
13. Scotti MM, Swanson MS. RNA mis-splicing in disease. Nat Rev Genet. 2016;17(1):19–32.
14. Mermoud JE, Cohen PT, Lamond AI. Regulation of mammalian spliceosome assembly by a protein phosphorylation mechanism. EMBO J. 1994;13(23):5679–88.
15. Amin EM, Oltean S, Hua J, Gammons MV, Hamdollah-Zadeh M, Welsh GI, et al. WT1 mutants reveal SRPK1 to be a downstream angiogenesis target by altering VEGF splicing. Cancer Cell. 2011;20(6):768–80.
16. Shultz JC, Goehe RW, Wijesinghe DS, Murudkar C, Hawkins AJ, Shay JW, et al. Alternative splicing of caspase 9 is modulated by the phosphoinositide 3-kinase/Akt pathway via phosphorylation of SRp30a. Cancer Res. 2010;70(22):9185–96.
17. Majumder B, Baraneedharan U, Thiyagarajan S, Radhakrishnan P, Narasimhan H, Dhandapani M, et al. Predicting clinical response to anticancer drugs using an ex vivo platform that captures tumour heterogeneity. Nat Commun. 2015;6:6169.
18. Radhakrishnan A, Nanjappa V, Raja R, Sathe G, Puttamallesh VN, Jain AP, et al. Corrigendum: a dual specificity kinase, DYRK1A, as a potential therapeutic target for head and neck squamous cell carcinoma. Sci Rep. 2017;7:46864.
19. Syed N, Chavan S, Sahasrabuddhe NA, Renuse S, Sathe G, Nanjappa V, et al. Silencing of high-mobility group box 2 (HMGB2) modulates cisplatin and 5-fluorouracil sensitivity in head and neck squamous cell carcinoma. Proteomics. 2015;15(2–3):383–93.
20. Radhakrishnan A, Nanjappa V, Raja R, Sathe G, Puttamallesh VN, Jain AP, et al. A dual specificity kinase, DYRK1A, as a potential therapeutic target for head and neck squamous cell carcinoma. Sci Rep. 2016;6:36132.
21. Subbannayya T, Leal-Rojas P, Barbhuiya MA, Raja R, Renuse S, Sathe G, et al. Macrophage migration inhibitory factor—a therapeutic target in gallbladder cancer. BMC Cancer. 2015;15:843.
22. Subbannayya Y, Syed N, Barbhuiya MA, Raja R, Marimuthu A, Sahasrabuddhe N, et al. Calcium calmodulin dependent kinase kinase 2—a novel therapeutic target for gastric adenocarcinoma. Cancer Biol Ther. 2015;16(2):336–45.
23. Cormier N, Yeo A, Fiorentino E, Paxson J. Optimization of the wound scratch assay to detect changes in murine mesenchymal stromal cell migration after damage by soluble cigarette smoke extract. J Vis Exp. 2015;106:e53414.
24. Schneider CA, Rasband WS, Eliceiri KW. NIH Image to ImageJ: 25 years of image analysis. Nat Methods. 2012;9(7):671–5.
25. Radhakrishnan P, Baraneedharan U, Veluchamy S, Dhandapani M, Pinto DD, Thiyagarajan S, et al. Inhibition of rapamycin-induced AKT activation elicits differential antitumor response in head and neck cancers. Cancer Res. 2013;73(3):1118–27.
26. Brijwani N, Jain M, Dhandapani M, Zahed F, Mukhopadhyay P, Biswas M, et al. Rationally co-targeting divergent pathways in KRAS wild-type colorectal cancers by CANscript technology reveals tumor dependence on Notch and Erbb2. Sci Rep. 2017;7(1):1502.
27. Tyanova S, Temu T, Sinitcyn P, Carlson A, Hein MY, Geiger T, et al. The Perseus computational platform for comprehensive analysis of (prote)omics data. Nat Methods. 2016;13(9):731–40.
28. Cho S, Hoang A, Sinha R, Zhong XY, Fu XD, Krainer AR, et al. Interaction between the RNA binding domains of Ser–Arg splicing factor 1 and U1-70K snRNP protein determines early spliceosome assembly. Proc Natl Acad Sci USA. 2011;108(20):8233–8.
29. Fu XD, Maniatis T. The 35-kDa mammalian splicing factor SC35 mediates specific interactions between U1 and U2 small nuclear ribonucleoprotein particles at the 3′ splice site. Proc Natl Acad Sci USA. 1992;89(5):1725–9.
30. Zhou Z, Fu XD. Regulation of splicing by SR proteins and SR protein-specific kinases. Chromosoma. 2013;122(3):191–207.
31. Mai S, Qu X, Li P, Ma Q, Cao C, Liu X. Global regulation of alternative RNA splicing by the SR-rich protein RBM39. Biochim Biophys Acta. 2016;1859(8):1014–24.
32. Hsu TY, Simon LM, Neill NJ, Marcotte R, Sayad A, Bland CS, et al. The spliceosome is a therapeutic vulnerability in MYC-driven cancer. Nature. 2015;525(7569):384–8.
33. Liu Y, Conaway L, Rutherford Bethard J, Al-Ayoubi AM, Thompson Bradley A, Zheng H, et al. Phosphorylation of the alternative mRNA splicing factor 45 (SPF45) by Clk1 regulates its splice site utilization, cell migration and invasion. Nucleic Acids Res. 2013;41(9):4949–62.
34. Zhang L, Yang H, Zhang W, Liang Z, Huang Q, Xu G, et al. Clk1-regulated aerobic glycolysis is involved in glioma chemoresistance. J Neurochem. 2017;142(4):574–88.
35. Muraki M, Ohkawara B, Hosoya T, Onogi H, Koizumi J, Koizumi T, et al. Manipulation of alternative splicing by a newly developed inhibitor of Clks. J Biol Chem. 2004;279(23):24246–544.
36. Edmond V, Merdzhanova G, Gout S, Brambilla E, Gazzeri S, Eymin B. A new function of the splicing factor SRSF2 in the control of E2F1-mediated cell cycle progression in neuroendocrine lung tumors. Cell Cycle. 2013;12(8):1267–78.
37. Razanau A, Xie J. Emerging mechanisms and consequences of calcium regulation of alternative splicing in neurons and endocrine cells. Cell Mol Life Sci. 2013;70(23):4527–36.
38. Radhakrishnan A, Nanjappa V, Raja R, Sathe G, Chavan S, Nirujogi RS, et al. Dysregulation of splicing proteins in head and neck squamous cell carcinoma. Cancer Biol Ther. 2016;17(2):219–29.
39. Harsha HC, Pandey A. Phosphoproteomics in cancer. Mol Oncol. 2010;4(6):482–95.

40. Wiredja DD, Ayati M, Mazhar S, Sangodkar J, Maxwell S, Schlatzer D, et al. Phosphoproteomics profiling of nonsmall cell lung cancer cells treated with a novel phosphatase activator. Proteomics. 2017;17(22):1700214.
41. Francavilla C, Lupia M, Tsafou K, Villa A, Kowalczyk K, Rakownikow Jersie-Christensen R, et al. Phosphoproteomics of primary cells reveals druggable kinase signatures in ovarian cancer. Cell Rep. 2017;18(13):3242–56.
42. Alli-Shaik A, Wee S, Lim LHK, Gunaratne J. Phosphoproteomics reveals network rewiring to a pro-adhesion state in annexin-1-deficient mammary epithelial cells. Breast Cancer Res. 2017;19(1):132.
43. Guo T, Lee SS, Ng WH, Zhu Y, Gan CS, Zhu J, et al. Global molecular dysfunctions in gastric cancer revealed by an integrated analysis of the phosphoproteome and transcriptome. Cell Mol Life Sci. 2011;68(11):1983–2002.
44. Lin LL, Huang HC, Juan HF. Discovery of biomarkers for gastric cancer: a proteomics approach. J Proteom. 2012;75(11):3081–97.
45. Zahari MS, Wu X, Pinto SM, Nirujogi RS, Kim MS, Fetics B, et al. Phosphoproteomic profiling of tumor tissues identifies HSP27 Ser82 phosphorylation as a robust marker of early ischemia. Sci Rep. 2015;5:13660.
46. Choi SY, Lin D, Gout PW, Collins CC, Xu Y, Wang Y. Lessons from patient-derived xenografts for better in vitro modeling of human cancer. Adv Drug Deliv Rev. 2014;79:222–37.
47. Damhofer H, Ebbing EA, Steins A, Welling L, Tol JA, Krishnadath KK, et al. Establishment of patient-derived xenograft models and cell lines for malignancies of the upper gastrointestinal tract. J Transl Med. 2015;13:115.
48. Borodovsky A, McQuiston TJ, Stetson D, Ahmed A, Whitston D, Zhang J, et al. Generation of stable PDX derived cell lines using conditional reprogramming. Mol Cancer. 2017;16(1):177.
49. Zhang T, Zhang L, Fan S, Zhang M, Fu H, Liu Y, et al. Patient-derived gastric carcinoma xenograft mouse models faithfully represent human tumor molecular diversity. PLoS One. 2015;10(7):e0134493.
50. Naro C, Sette C. Phosphorylation-mediated regulation of alternative splicing in cancer. Int J Cell Biol. 2013;2013:151839.
51. Colwill K, Pawson T, Andrews B, Prasad J, Manley JL, Bell JC, et al. The Clk/Sty protein kinase phosphorylates SR splicing factors and regulates their intranuclear distribution. EMBO J. 1996;15(2):265–75.
52. Bonomi S, Gallo S, Catillo M, Pignataro D, Biamonti G, Ghigna C. Oncogenic alternative splicing switches: role in cancer progression and prospects for therapy. Int J Cell Biol. 2013;2013:962038.
53. Bemmo A, Dias C, Rose AA, Russo C, Siegel P, Majewski J. Exon-level transcriptome profiling in murine breast cancer reveals splicing changes specific to tumors with different metastatic abilities. PLoS One. 2010;5(8):e11981.
54. Araki S, Dairiki R, Nakayama Y, Murai A, Miyashita R, Iwatani M, et al. Inhibitors of CLK protein kinases suppress cell growth and induce apoptosis by modulating pre-mRNA splicing. PLoS One. 2015;10(1):e0116929.
55. Li P, Carter G, Romero J, Gower KM, Watson J, Patel NA, et al. Clk/STY (cdc2-like kinase 1) and Akt regulate alternative splicing and adipogenesis in 3T3-L1 pre-adipocytes. PLoS One. 2013;8(1):e53268.
56. ElHady AK, Abdel-Halim M, Abadi AH, Engel M. Development of selective Clk1 and -4 inhibitors for cellular depletion of cancer-relevant proteins. J Med Chem. 2017;60(13):5377–91.
57. Fedorov O, Huber K, Eisenreich A, Filippakopoulos P, King O, Bullock AN, et al. Specific CLK inhibitors from a novel chemotype for regulation of alternative splicing. Chem Biol. 2011;18(1):67–766.
58. Eisenreich A, Zakrzewicz A, Huber K, Thierbach H, Pepke W, Goldin-Lang P, et al. Regulation of pro-angiogenic tissue factor expression in hypoxia-induced human lung cancer cells. Oncol Rep. 2013;30(1):462–70.
59. Mavrou A, Brakspear K, Hamdollah-Zadeh M, Damodaran G, Babaei-Jadidi R, Oxley J, et al. Serine–arginine protein kinase 1 (SRPK1) inhibition as a potential novel targeted therapeutic strategy in prostate cancer. Oncogene. 2015;34(33):4311–9.
60. Cao W, Jamison SF, Garcia-Blanco MA. Both phosphorylation and dephosphorylation of ASF/SF2 are required for pre-mRNA splicing in vitro. RNA. 1997;3(12):1456–67.
61. Chanseok Shin JLM. The SR protein SRp38 represses splicing in M phase cells. Cell. 2002;111(3):10.

Affiliations

Niraj Babu[1,2] · Sneha M. Pinto[1,3] · Manjusha Biswas[4] · Tejaswini Subbannayya[1,4] · Manoj Rajappa[4] · Sonali V. Mohan[1,2] · Jayshree Advani[1] · Pavithra Rajagopalan[1] · Gajanan Sathe[1] · Nazia Syed[1] · Vinod D. Radhakrishna[4] · Oliyarasi Muthusamy[4] · Sanjay Navani[5] · Rekha V. Kumar[6] · Gopal Gopisetty[7] · Thangarajan Rajkumar[7] · Padhma Radhakrishnan[8] · Saravanan Thiyagarajan[4] · Akhilesh Pandey[1,2,9,10,11] · Harsha Gowda[1,2,12] · Pradip Majumder[8] · Aditi Chatterjee[1,2,4]

1 Institute of Bioinformatics, International Technology Park, Bangalore, Bangalore 560066, India

2 Manipal Academy of Higher Education, Manipal 576104, India

3 Center for Systems Biology and Molecular Medicine, Yenepoya (Deemed To Be University), Mangalore 575018, India

4 Mitra Biotech, Bangalore 560100, India

5 Lab Surgpath, Mumbai 400034, India

6 Department of Pathology, Kidwai Memorial Institute of Oncology, Bangalore 560029, India

7 Department of Molecular Oncology, Cancer Institute (WIA), Chennai 600020, India

8 Mitra Biotech, Woburn, MA 01801, USA

9 Department of Laboratory Medicine and Pathology, Mayo Clinic, Rochester, MN 55905, USA

[10] Center for Individualized Medicine, Mayo Clinic, Rochester, MN 55905, USA

[11] Center for Molecular Medicine, National Institute of Mental Health and Neurosciences (NIMHANS), Hosur Road, Bangalore 560029, India

[12] Cancer Precision Medicine, QIMR Berghofer, Royal Brisbane Hospital, Brisbane, QLD 4029, Australia